Methionine Oxidation Inhibits Assembly and Promotes Disassembly of Apolipoprotein C-II Amyloid Fibrils[†]

Katrina J. Binger,*[,‡,§] Michael D. W. Griffin,[‡] and Geoffrey J. Howlett[‡]

Department of Biochemistry and Molecular Biology, Bio21 Molecular Science and Biotechnology Institute, The University of Melbourne, Parkville, Victoria 3010, Australia, and CSIRO Molecular and Health Technologies, 343 Royal Pde, Parkville, Victoria 3010, Australia

Received May 19, 2008; Revised Manuscript Received July 29, 2008

ABSTRACT: Methionine residues are linked to the pathogenicity of several amyloid diseases; however, the mechanism of this relationship is largely unknown. These diseases are characterized, *in vivo*, by the accumulation of insoluble proteinaceous plaques, of which the major constituents are amyloid fibrils. *In vitro*, methionine oxidation has been shown to modulate fibril assembly in several well-characterized amyloid systems. Human apolipoprotein (apo) C-II contains two methionine residues (Met-9 and Met-60) and readily self-assembles *in vitro* to form homogeneous amyloid fibrils, thus providing a convenient system to examine the effect of methionine oxidation on amyloid fibril formation and stability. Upon oxidation of the methionine residues of apoC-II with hydrogen peroxide, fibril formation was inhibited. Oxidized apoC-II molecules did not inhibit native apoC-II assembly, indicating that the oxidized molecules had a reduced ability to interact with the growing fibrils. Single Met-Val substitutions were performed and showed that oxidation of Met-60 had a more significant inhibitory effect than oxidation of Met-9. In addition, Met-Gln substitutions designed to mimic the effect of oxidation on side chain hydrophilicity showed that a change in hydrophobicity at position 60 within the core region of the fibril had a potent inhibitory effect. The oxidation of preformed apoC-II fibrils caused their dissociation; however, mutants in which the Met-60 was substituted with a valine were protected from this peroxide-induced dissociation. This work highlights an important role for methionine in the formation of amyloid fibril structure and gives new insight into how oxidation affects the stability of mature fibrils.

The oxidation of proteins is associated with both natural aging and several disease processes (*1*). Methionine is one of the most easily oxidized amino acids and is converted to methionine sulfoxide or sulfone derivatives by many different mechanisms, such as hydrogen peroxide treatment, metal-catalyzed reactions, and UV exposure (*2*). In all cell types the oxidative state of methionine is regulated by methionine sulfoxide reductases (MsrA and MsrB2 in humans (*3, 4*), which specifically reduce oxidized forms of methionine. This reaction is proposed to regulate the life span of mammals, insects, and yeast (*5*) with deletion of the *MSRA* gene in mice resulting in a 40% reduced life span (*6*). Specific roles for oxidized methionines *in vivo* are yet to be resolved, but in general, methionine residues are proposed to act, in part, as endogenous antioxidants to protect cells from the accumulation of reactive oxygen species (ROS)[1] (*7*). In many studies, methionine oxidation has been shown to result in a loss of protein activity; for example, in α1-antitrypsin, methionine oxidation induced by smoking results in loss of activity and the development of pulmonary emphysema (*8*). The amount of oxidized protein is also proposed to reflect the balance of oxidant and antioxidant reactions in the cell, where accumulation of oxidized proteins is an indicator of the extent of oxidative damage (*1*).

One class of diseases in which oxidative damage is found extensively is the amyloid diseases (*9*). Amyloid diseases are characterized by the accumulation of insoluble amyloid deposits of which the major constituents are amyloid fibrils (*10, 11*). To date, more than 25 proteins have been shown to assemble into amyloid fibrils *in vivo* with subsequent accumulation of these fibrils, either intra- or extracellularly, ultimately resulting in the development of diseases such as Alzheimer's disease (AD), transmissible spongiform encephalopathies or prion diseases, and adult-onset (type II) diabetes (*12*−*14*). The main pathogenic mechanism for AD is the misprocessing of amyloid precursor protein (APP) and subsequent accumulation and aggregation of a 41−43-residue peptide (Aβ) (*15*). However, more recent studies suggest that soluble prefibrillar oligomers are the more toxic or disease-causing species (*16, 17*). Post-mortem analysis of AD brains has shown high levels of protein oxidation, lipid peroxidation, and oxidative damage to mitochondria, indicating that oxidative stress is a characteristic of AD (*18, 19*). The oxidative state of the Aβ peptide is proposed to be critical

[†] This work was supported by the Australian Research Council (Grant DP0449510) and the National Health and Medical Research Council of Australia (Grant 350229).

* Address correspondence to this author at the University of Melbourne. Tel: 61-3-8344-2274. Fax: 61-3-9348-1421. E-mail: katrinabinger@gmail.com.

[‡] The University of Melbourne.

[§] CSIRO Molecular and Health Technologies.

[1] Abbreviations: Aβ, amyloid-β peptide; AD, Alzheimer's disease; apo, apolipoprotein; GuHCl, guanidine hydrochloride; Msr, methionine sulfoxide reductase; OX, oxidized; PrP, prion protein; ROS, reactive oxygen species; ThT, thioflavin T.

10.1021/bi8009339 CCC: $40.75
Published on Web 08/26/2008

to its neurotoxic properties *in vivo* (*20*) where the single methionine at position 35 is proposed to be involved in the generation of ROS (*21*). Also, MsrA activity has been shown to be significantly reduced in AD brains compared to age-matched control subjects, further implicating methionine oxidation in Alzheimer's disease pathogenesis (*22*).

Amyloid fibrils are characterized by a common core cross-β structure suggesting that the large number of different proteins shown to form amyloid fibrils assemble *via* a common pathway and, thus, have a common pathological mechanism (*23*). Numerous studies have sought to detect similarities between amyloid-forming proteins (*24*−*26*); however, due to low sequence identity and lack of native structure homology, predicting the propensity and mechanism of aggregation of these proteins has proved a great challenge (*10*). Interestingly, methionine oxidation appears to be a common modulator of fibril formation and has been shown to inhibit the aggregation of Aβ (*27*), prion protein (PrP) (*28*), transthyretin (*29*), and α-synuclein (*30*). Additionally, the susceptibility or aggressiveness of several amyloid diseases is significantly affected by the presence of a methionine in the primary sequence of the protein. This is particularly evident in the case of the human prion disease, variant Cruetzfelt−Jakob disease (vCJD), where, in all reported cases of the disease, patients are found to be homozygous for methionine at position 129 of the *PNRP* gene which encodes PrP (*31, 32*). Also, in a recent study with a 21-residue PrP peptide, Bergstrom et al. have shown that while methionine oxidation reduces fibrillization tendencies, the neurotoxic effect of the oxidized peptide *in vivo* is slightly increased (*33*).

In this study we have investigated the effect of methionine oxidation on the formation and stability of mature human apolipoprotein (apo) C-II amyloid fibrils. ApoC-II (8.9 kDa) is one of several apolipoproteins identified in atherosclerotic plaques *in vivo* (*34*) and is found colocalized in human coronary artery plaques with serum amyloid P, a universal constituent of amyloid deposits (*35*). ApoC-II fibrils formed *in vitro* are homogeneous when viewed by electron microscopy and display a characteristic X-ray diffraction pattern, indicating the formation of cross-β structure (*36*). A unique property of mature apoC-II fibrils is that they are relatively small and remain soluble, allowing characterization of fibril formation by analytical ultracentrifugation where we have shown the mature fibrils to assemble via a reversible pathway that includes fibril breaking and joining (*37*). On the basis of these extensive kinetic studies of the apoC-II amyloid fibril system it came as a surprise that a preparation of apoC-II with both methionines oxidized was unable to form fibrils. Here, we have used site-directed mutagenesis to extend this initial observation and explore the basis for the inhibition of fibril formation by methionine oxidation. We show that a change in hydrophobicity of a single residue in a core fibril region of apoC-II is responsible for a significant reduction in fibril assembly. In addition, we have explored the potential of using methionine oxidation to reverse apoC-II fibril assembly and show that treatment of preformed fibrils with hydrogen peroxide dissociates the monomer in a time-dependent manner. This study highlights an important role of methionine oxidation in regulating the stability of preformed amyloid fibrils.

EXPERIMENTAL PROCEDURES

Materials. Hydrogen peroxide was purchased from Merck (Darmstadt, Germany). Thioflavin T was purchased from Sigma (St. Louis, MO). The peptides apoC-II$_{56-76}$ (STAAM-STYTGIFTDQVLSVLK) and apoC-II$_{60-70}$ (MSTYTGIFT-DQ) were synthesized by Dr. Dennis Scanlon (Bio21 Molecular Science and Biotechnology Institute). An oxidized preparation of wild-type apoC-II was kindly donated by Ms. Leanne Wilson.

Mutagenesis, Expression, and Purification of ApoC-II. Wild-type and mutant apoC-II were expressed in *Escherichia coli* BL21(DE3) cell lines transformed with a pET-11a expression vector containing human apoC-II cDNA. All mutants (M9V, M60V, M9V/M60V, M9Q, M60Q, M9Q/M60Q) were constructed using the QuikChange method according to the manufacturer's protocol (Stratagene, La Jolla, CA). Mutations in the apoC-II gene were verified by DNA sequencing (Applied Genetic Diagnostics, Victoria, Australia), and multiple rounds of QuikChange mutagenesis were performed if necessary to construct double mutants (M9V/M60V and M9Q/M60Q). The mutated DNA was isolated and purified by miniprep (Qiagen Inc., MD) and then transformed into *E. coli* BL21(DE3) for expression and purification as described previously (*36, 38*). The molecular masses of wild-type and mutant apoC-II preparations were confirmed on a Q-TOF LC mass spectrometer (Agilent Technologies Inc., DE). Purified wild-type and mutant apoC-II preparations were stored as 30−40 mg/mL stocks in 5 M GuHCl and 10 mM Tris-HCl, pH 8.0, to prevent aggregation at −20 °C.

High-Performance Liquid Chromatography. Analyses of unoxidized and oxidized apoC-II preparations were examined by loading 1 mL solutions onto a butyl (C4) 300 Å aquapore HPLC column eluted with a 90% acetonitrile gradient at a constant flow rate of 3 mL/min. Oxidized apoC-II eluted ∼70 s earlier than unoxidized, allowing convenient purification.To determine the percentage of oxidized material over time, the HPLC profiles were fit to a multiple Gaussian model using the program "PeakFit" to estimate the area under each peak. The amount of unoxidized protein (elution time ∼37.1 min) at each time point was subtracted from the amount at time zero to calculate the percentage of oxidized protein.

Preparation of Oxidized ApoC-II. Oxidized wild-type and mutant apoC-II were prepared by incubating 1 mg of protein with 0.1% H_2O_2 for 16 h in 100 mM sodium phosphate, pH 7.4, at room temperature. The samples were then purified by HPLC with a butyl (C4) column, as described above. Fractions collected from the HPLC column containing oxidized protein were lyophilized and stored as stocks of 15−30 mg/mL in 5 M GuHCl and 10 mM Tris-HCl, pH 8. The molecular mass of each oxidized preparation was confirmed with a Q-TOF LC mass spectrometer (Agilent Technologies Inc., DE).

Thioflavin T Fluorescence Measurements. Fibril formation by wild-type and mutant apoC-II was initiated by diluting apoC-II stocks (30−40 mg/mL) into refolding buffer (100 mM sodium phosphate, pH 7.4, 0.1% sodium azide) and incubating at room temperature at a final concentration of 0.3 mg/mL (33 μM), unless noted otherwise. Fibril samples which were subsequently treated with hydrogen peroxide were formed in this manner for 7 days, after which hydrogen

peroxide was added to a final concentration of 0.1% and incubated at room temperature for a further 72 h. Concentrated stocks of apoC-II$_{60-70}$ and apoC-II$_{56-76}$ (~20 mg/mL) were maintained in 5 M GuHCl and 10 mM Tris-HCl, pH 8.0 at −20 °C. Fibril formation was initiated by dilution of these stocks to 0.3 mg/mL apoC-II$_{60-70}$ or 0.5 mg/mL apoC-II$_{56-76}$ peptide in refolding buffer at room temperature. To monitor fibril assembly, at the required time points 20 μL aliquots of sample were added to 220 μL of 8 μM ThT in refolding buffer. Fluorescence intensities were measured in duplicate using an f_{max} fluorescence plate reader (Molecular Devices, Sunnyvale, CA) with excitation and emission filters of 444 and 485 nm, respectively. Control measurements were performed with a 0.1 mg/mL sample of bovine serum albumin (Sigma, St. Louis, MO) which was incubated at room temperature in refolding buffer with ThT fluorescence measurements as per the apoC-II procedure. These control readings were then subtracted from the measured ThT fluorescence of the apoC-II sample to give a baseline corrected ThT fluorescence.

Pelleting Assay. Fibril formation was initiated as described previously, and at the selected time points, aliquots of 100 μL were removed and subjected to centrifugation at 100000 rpm (TL-100 rotor, Beckman) for 30 min at 4 °C. Under these centrifugation conditions monomeric apoC-II does not sediment significantly. The concentration of monomeric apoC-II in the supernatant after centrifugation was monitored using fluorescence measurements based on the reaction of fluorescamine with primary amine groups (*39*). The supernatants (90 μL) were added to a microtiter plate containing 75 μL of refolding buffer and 75 μL of 0.5 mg/mL fluorescamine in acetonitrile. Samples were incubated at room temperature for 5 min, and fluorescence intensities were measured using an f_{max} fluorescence plate reader (Molecular Devices, Sunnyvale, CA) with excitation and emission filters of 355 and 460 nm, respectively.

Mass Spectrometry. Samples (100 μL) were dialyzed into 10 mM ammonium acetate with MINI dialysis units (Pierce Biotechnology Inc., IL) with several buffer changes. An aliquot (10 μL) of each sample was saved, and the remaining sample was subjected to centrifugation at 100000 rpm in a Beckman OptimaMax centrifuge to separate free monomer from the fibrils. Pellets were resuspended in 20 μL of 10 mM ammonium acetate, and 10 μL of each sample (total, pellet and supernate) was injected into a Q-TOF LC mass spectrometer (Agilent Technologies Inc., DE) operating with a capillary voltage of 5 kV, a skimmer voltage of 65 V, and a fragmentor voltage at 350 V. All deconvoluted mass spectra are presented with normalized intensities.

Analytical Ultracentrifugation. Sample (280 μL) and reference (300 μL) solutions were centrifuged at 8000 rpm for 280 min at 20 °C with a An-60 Ti rotor in a XL-I analytical ultracentrifuge (Beckman Coulter, Inc., CA). Radial absorbance data were collected at a wavelength of 280 nm with radial increments of 0.002 cm with radial scans taken in 8 min intervals. Sedimentation velocity profiles of apoC-II fibrils were analyzed with the program SEDFIT using the c(S) model (*40*), with the hydrodynamic scaling law derived on the basis of a worm-like chain model and a relation between sedimentation coefficient and fibril molecular weight as described previously (*41*). Analysis of experimental data was performed with second derivative Tikhonov−Phillips regularization (*42*) due to the broad size distribution of apoC-II fibrils. A regularization parameter of $p = 0.68$ was used with 150 sedimentation coefficient increments. Time-independent (TI) noise and the sample meniscus position were fitted. The weight-average sedimentation coefficients of the samples were calculated by integration of the sedimentation distributions over a specific range.

RESULTS

Methionine Oxidation Affects ApoC-II Fibril Formation. We have previously shown that apoC-II readily assembles into amyloid fibrils under physiological pH and without the need for high temperature or agitation (*36*). Thus, it came as a surprise when a recombinant preparation of apoC-II was found to have a significantly reduced ability to form amyloid fibrils. This preparation was free from contaminants when analyzed by SDS−PAGE (data not shown), and we subsequently looked for chemical modifications as a possible cause for the variability. The fibril incompetent and control preparation of apoC-II (which readily forms amyloid fibrils) were diluted to 79 μM and loaded on a butyl HPLC column (Figure 1A). When compared with the control, the HPLC trace of the incompetent preparation has three discrete peaks (elution times: peak 1, 34.7 min; peak 2, 35.8 min; peak 3, 37.0 min). The three peaks were analyzed by mass spectrometry (Figure 1B). Peak 3 had a mass of 8915 Da, corresponding to nonoxidized apoC-II. Peaks 2 and 1 had additional masses of 16 and 32 Da, respectively. Tandem MS/MS revealed these additional masses to correspond to apoC-II with one and both methionines oxidized, respectively (data not shown). Small abundance peaks with additional masses of 23 and 39 Da were also detected, which can be attributed to the presence of sodium and potassium adducts of apoC-II, respectively. To assess if methionine oxidation was the cause of the variation in amyloid formation, the three fractions were purified, and their capacity to form fibrils at a concentration of 33 μM was monitored by ThT fluorescence (Figure 1C). The unpurified preparation showed no significant increase in ThT fluorescence over the time course, as expected. The fraction corresponding to peak 3 showed a significant increase in ThT fluorescence over the time course indicating amyloid fibril formation. The presence of apoC-II amyloid fibrils with normal morphology was also confirmed by electron microscopy (data not shown). Fractions corresponding to peaks 2 and 1 showed no significant change in ThT fluorescence over the time course, indicating that apoC-II with one or both methionines oxidized does not form fibrils under these conditions. To investigate if oxidized apoC-II was completely inhibited from forming amyloid fibrils, we performed a ThT assay at high protein concentrations (112 μM), where apoC-II fibril formation is greatly favored (see Supporting Information). Under these conditions, oxidized apoC-II showed an increase in ThT fluorescence after a significant delay of 72 h, indicating that the ability to form fibrils is significantly impaired.

Methionine-Oxidized ApoC-II Does Not Inhibit Nonoxidized Fibril Assembly. A coincubation of oxidized apoC-II and nonoxidized apoC-II was performed to assess if oxidized apoC-II could interact with and possibly inhibit fibril formation. Oxidized apoC-II was added in 0.5:1, 1:1, and 2:1 molar ratios to nonoxidized apoC-II and assayed by ThT

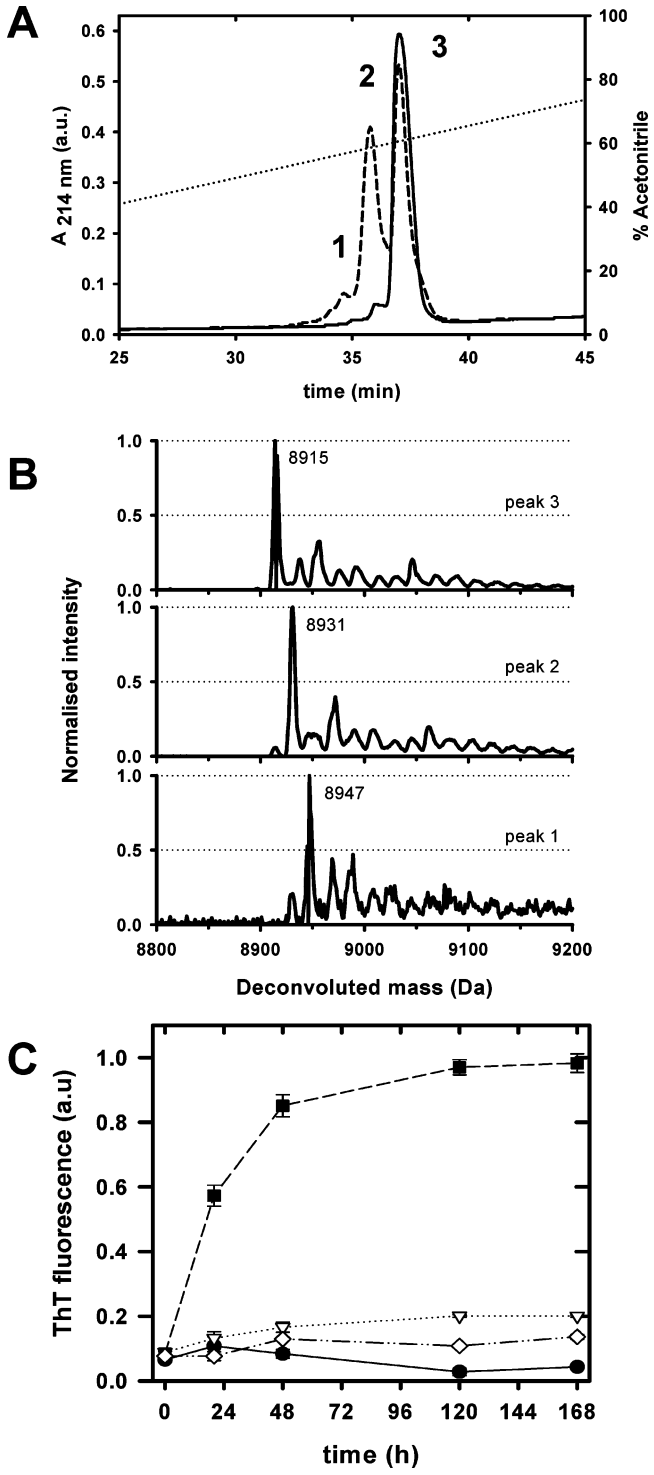

FIGURE 1: Effect of methionine oxidation on amyloid fibril formation by apoC-II. Panel A: HPLC trace of oxidized (dashed line) and unoxidized (solid line) apoC-II eluted with a 90% acetonitrile gradient (dotted line) on a 300 Å butyl column. Panel B: Each peak from the HPLC trace was purified and analyzed by mass spectrometry. The deconvoluted mass spectrum of each peak is shown with a normalized intensity. Panel C: Thioflavin T fluorescence of purified peak 1 (closed circles), peak 2 (open triangles), peak 3 (closed squares), and the unpurified sample (open diamonds) at a concentration of 33 μM protein.

fluorescence over time (Figure 2A). Even at 2:1 molar ratios of oxidized:nonoxidized protein, fibril formation was not inhibited and was even slightly increased. To investigate if the oxidized protein was interacting with nonoxidized apoC-II and becoming incorporated into the amyloid fibrils, the samples were subjected to centrifugation to separate the fibrils (pellet) from the monomer (supernate) and analyzed separately by mass spectrometry (Figure 2B). For the control sample of apoC-II fibrils alone, the pellet and supernate fractions were essentially identical and only contained nonoxidized apoC-II with a molecular mass of 8915 Da. For the sample incubated with an equimolar concentration of oxidized apoC-II, nonoxidized apoC-II was identified in the pellet fraction, and primarily oxidized apoC-II (8947 Da) was detected in the supernate. A small amount of oxidized apoC-II was also present in the pellet fraction, suggesting some incorporation into the fibrils; however, this did not inhibit fibril assembly.

Oxidation of Methionine within the ApoC-II Core Fibril Region Inhibits Fibril Formation. Previous studies in our laboratory have identified two regions of the apoC-II sequence that constitute the hydrophobic core of mature apoC-II amyloid fibrils (*43*). ApoC-II contains two methionine residues within its primary sequence (Met-9 and Met-60), with the methionine at position 60 located within one of the core fibril regions (Figure 3A). To assess if the oxidation of one particular methionine residue affected the fibrillogenesis of apoC-II more than the other, single methionine-valine mutations were made (M9V and M60V). The remaining methionine residue in each of these mutants was then oxidized by treatment with hydrogen peroxide, and the V9/M60^{ox} and M9^{ox}/V60 preparations were purified and assayed for their fibril forming capacity. Figure 3B shows the ThT fluorescence of nonoxidized and oxidized wild type and Met-Val mutants over time. For both V9/M60^{ox} and oxidized wild-type apoC-II (M9^{ox}/ M60^{ox}), there was no significant increase in ThT fluorescence over time. In contrast, there is a small increase in ThT fluorescence observed in the M9^{ox}/V60 sample, indicating that fibril formation was not completely inhibited by the oxidation of Met-9. Nonoxidized M9V and M60V mutants assembled into fibrils with similar kinetics to wild type (panel B, solid squares and triangles, respectively), suggesting that these methionine residues are not essential to apoC-II fibril formation. To further probe the effect of Met-60 oxidation on apoC-II assembly, we utilized two peptides that constitute the core apoC-II fibril region (apoC-II$_{60-70}$ and apoC-II$_{56-76}$). As previously reported (*43*), both peptides readily assemble into amyloid fibrils. However, oxidation of these peptides blocked their ability to form fibrils (Figure 3C,D), again demonstrating the importance of Met-60 in the formation of the apoC-II core fibril structure.

A Change in Hydrophobicity of a Single Residue within the Core Region Inhibits Fibril Formation. The addition of an oxygen molecule to the sulfur of a methionine residue effectively increases the hydrophilicity of the side chain. We set out to determine if the reason behind the inability of methionine-oxidized apoC-II to assemble into fibrils was due to this single-residue change in hydrophobicity in the core region of the fibrils or if methionine residues play an important role in driving the folding of monomeric apoC-II into a fibril-competent structure. A series of single and double methionine-glutamine substitutions were made (M9Q, M60Q, and M9Q/M60Q) to mimic the effect of oxidation, and the fibril-forming ability of these mutants was evaluated by ThT fluorescence (Figure 4). Under conditions in which wild-type apoC-II readily assembles into amyloid fibrils (33 μM

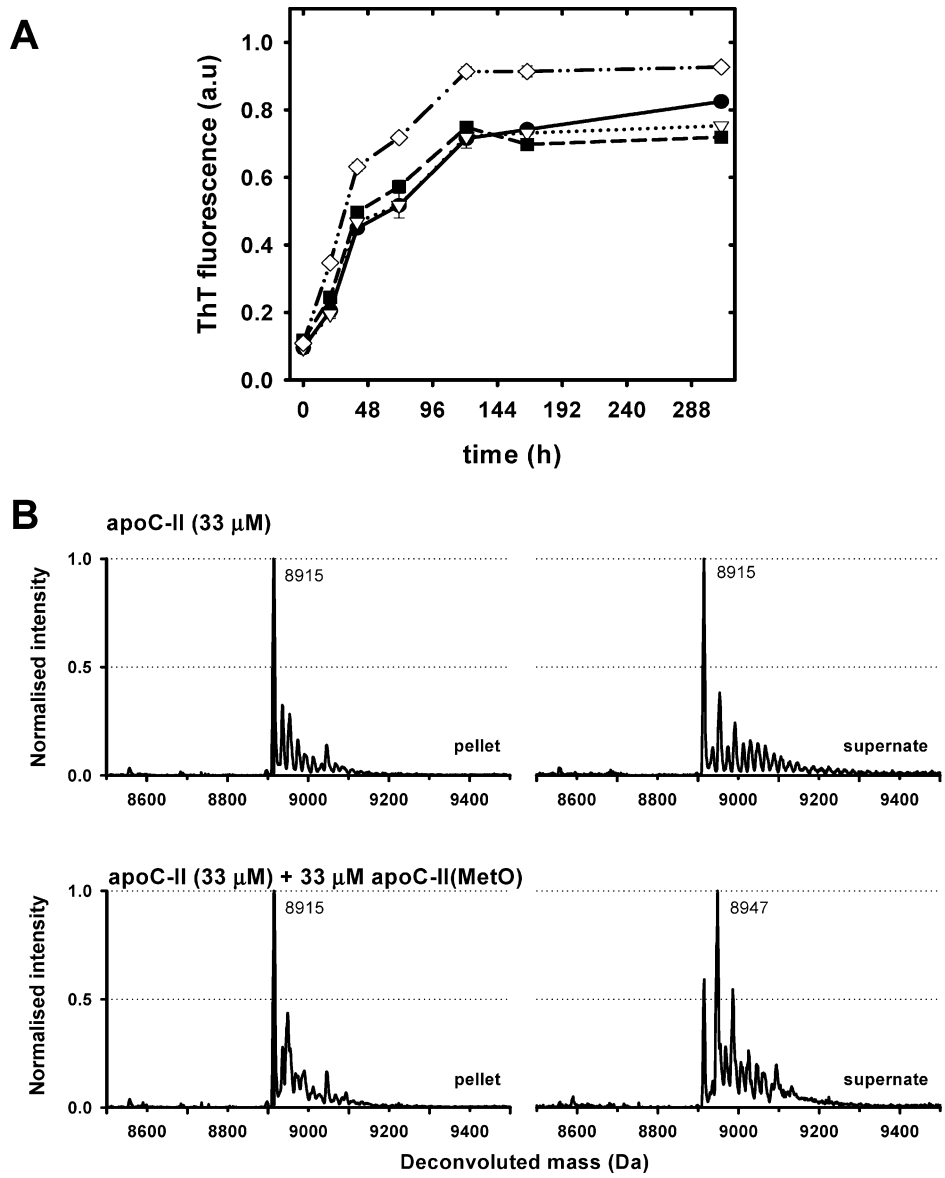

FIGURE 2: Effect of increasing concentrations of oxidized apoC-II on fibril formation by wild-type apoC-II. Panel A: 33 μM apoC-II was incubated at room temperature in the presence of 0 μM (closed circles), 16 μM (open triangles), 33 μM (closed squares), and 67 μM (open diamonds) oxidized apoC-II and monitored by thioflavin T fluorescence over time. Panel B: Following incubation of 33 μM apoC-II alone (0 μM) or with 33 μM oxidized apoC-II for 168 h, the samples were centrifuged to separate the fibrils (pellet) from the monomer (supernate) and analyzed separately by mass spectrometry. The deconvoluted mass spectrum of each pellet and supernate is shown with a normalized intensity.

apoC-II, 100 mM sodium phosphate, pH 7.4), mutants in which a glutamine was substituted at position 60 did not show any significant increase in ThT fluorescence over the time period (Figure 4A). In contrast, the mutant with a glutamine substituted only at position 9 formed fibrils with relatively similar kinetics to wild-type apoC-II. Circular dichroism spectroscopy studies to compare the secondary structure of the wild type and glutamine-substituted mutants showed no significant difference. Each displayed a characteristic spectral minimum at 202 nm, indicating a predominantly disordered structure (see Supporting Information). To assess if the Gln-60 mutants were completely inhibited from fibril formation, ThT assays were set up at high initial monomeric concentration (112 μM) where apoC-II fibril formation is rapid (Figure 4B). Under these conditions, Gln-60 mutants showed a significant delay in fibril formation when compared to wild type but were not completely inhibited. The fibril morphology of each mutant was evaluated by electron microscopy and did not show any detectable difference compared to those fibrils formed from wild-type apoC-II (data not shown). This shows that a change in hydrophobicity at a single position in the apoC-II core region is sufficient to significantly reduce the fibril-forming ability of this protein.

Dissociation of Fibrils by Hydrogen Peroxide Treatment. Our previous work has shown that apoC-II amyloid fibrils assemble via a reversible pathway that includes reversible dissociation of monomer and fibril breaking and rejoining as integral steps of the pathway (*37*). A key observation of this work is that apoC-II fibrils are in a reversible equilibrium with a free pool of monomer. In addition, the size of this free pool increases when fibrils are diluted. We sought to determine if methionine oxidation also reversed or dissociated preformed apoC-II fibrils. We considered that this may occur as a result of either oxidizing accessible methionine residues within the core or at the ends of the fibrils or

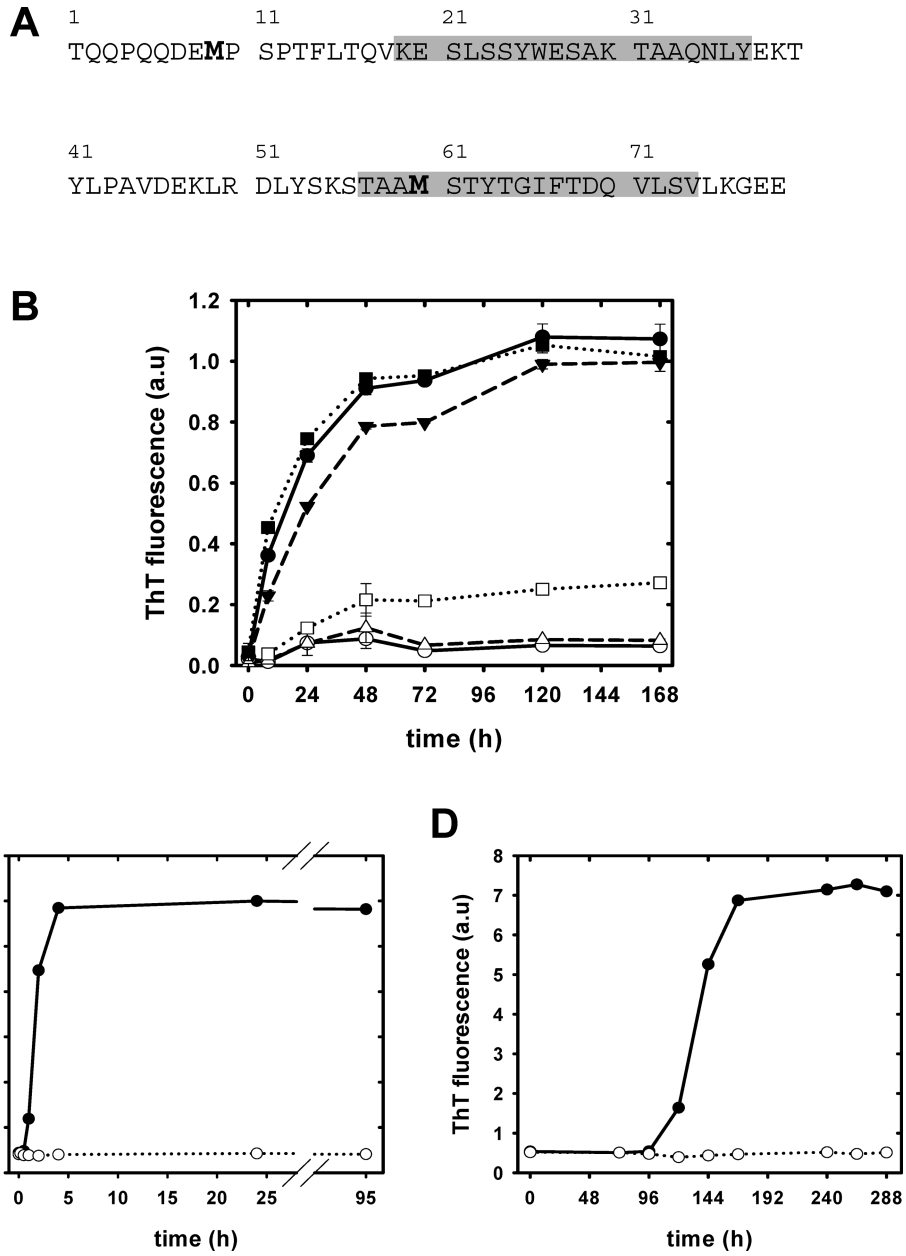

FIGURE 3: Site-specific effect of methionine oxidation on apoC-II fibril assembly. Panel A: Primary sequence of apoC-II with the amyloid structural core region highlighted in gray (*41*) and the methionines at positions 9 and 60 in bold. Panel B: Thioflavin T fluorescence over time of unoxidized (closed symbols) and oxidized (open symbols) apoC-II wild type and Met-Val mutant fibril formation. Key: Wild type (circles), M9V (triangles), and M60V (squares). Panels C and D: Thioflavin T fluorescence over time of unoxidized (closed circles) and oxidized (open circles) amyloidogenic peptides apoC-II$_{60-70}$ (panel C) and apoC-II$_{56-76}$ (panel D).

oxidizing the free monomer pool and subsequently causing a shift in the fibril−monomer equilibrium resulting in fibril dissociation. Wild type and the double valine mutant (M9V/M60V) were incubated at 33 μM in refolding buffer at room temperature for 7 days to allow fibril formation to occur. The fibril formation process was monitored by both ThT fluorescence and a pelleting assay and showed that after 7 days fibril formation had plateaued with $\sim$ 6% free monomeric apoC-II (data not shown). At this time, hydrogen peroxide was added to the fibril solutions to a final concentration of 0.1%, and the samples were incubated for a further 72 h. An aliquot of each fibril solution was removed prior to addition of hydrogen peroxide and left untreated as a control. The treated samples were then monitored by ThT fluorescence and a pelleting assay to detect any changes in the free monomeric pool over time. Figure 5 shows the change in ThT fluorescence and free monomer over time for wild-type (panels A and C) and M9V/M60V (panels B and D) fibrils. Treatment of preformed wild-type apoC-II fibrils with hydrogen peroxide results in a significant decrease in ThT fluorescence which corresponds with an increase in free monomer to $\sim$16%. In contrast, M9V/M60V fibrils show no significant change in ThT fluorescence or free monomer over the same time period.

Sedimentation velocity experiments were performed to determine if the hydrogen peroxide treatment was simply causing fibril dissociation or also inducing fibril breaking. Fibril samples that were incubated with 0.1% hydrogen peroxide for 72 h were centrifuged at 8000 rpm with radial scans taken at 8 min intervals for 480 min. Under these conditions only apoC-II fibrils sediment while monomeric apoC-II remains as nonsedimenting material, thus allowing

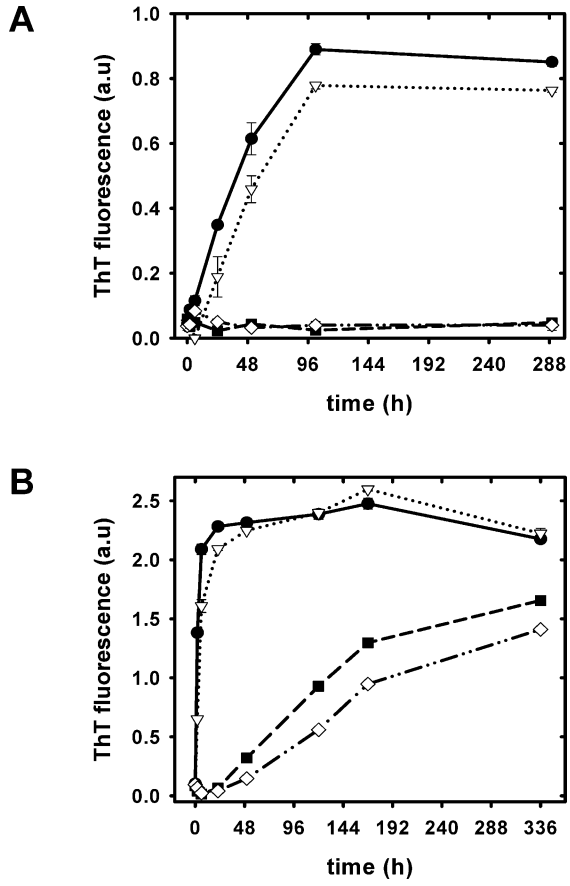

FIGURE 4: Effect of change in hydrophobicity on fibril formation by apoC-II. ThT fluorescence of wild type and Met-Gln mutants incubated at 33 μM (panel A) and 112 μM (panel B) for wild type (closed circles), M9Q (open triangles), M60Q (closed squares), and M9Q/M60Q (open diamonds).

simultaneous analysis of the size of the fibrils and free monomeric pool. The raw sedimentation data were fit to the c(S) model with the sedimentation coefficient distributions shown in Figure 6. The modal sedimentation coefficient of the wild-type (panel A) and M9V/M60V (panel B) fibrils did not significantly change after treatment with hydrogen peroxide, with a decrease in the weight-average sedimentation coefficient of 16 and 5 S, respectively. Wild-type fibrils treated with hydrogen peroxide show a decrease in the amount of sedimenting fibrils of 16% (panel A), in agreement with the pelleting assay (Figure 5) that showed an increase in free monomer in these samples. M9V/M60V fibrils that were treated with hydrogen peroxide were relatively similar to control untreated fibril samples with a decrease in the amount of sedimenting fibrils of only 6%, suggesting that the hydrogen peroxide did not affect the sedimentation of these fibrils and that the decrease observed in the wild-type sample is a result of the specific oxidation of methionine residues within apoC-II fibrils.

Mechanism for Hydrogen Peroxide Induced Dissociation of Preformed ApoC-II Fibrils. To determine the mechanism by which apoC-II fibrils are dissociated by hydrogen peroxide, we wanted to ascertain how accessible the methionines within the fibrils were by comparing the rate of oxidation between fibrillar and monomeric apoC-II. Samples of monomeric apoC-II were incubated in the presence of 0.1% hydrogen peroxide and analyzed by HPLC at several time points. Samples of fibrillar apoC-II were first incubated at 33 μM in refolding buffer for 7 days to ensure fibril formation was complete, before treatment with hydrogen peroxide and HPLC analysis as per the monomer samples. The percentage of oxidized protein is plotted versus time in Figure 7. The monomeric wild-type apoC-II was readily oxidized to ~80% completion after incubation with hydrogen peroxide for only 1 h and is completely oxidized after 6 h. In comparison, fibrillar wild-type apoC-II is somewhat protected from this treatment, with only ~32% oxidized after 1 h with complete oxidation achieved only after incubation with hydrogen peroxide for 72 h. The experiments were repeated with M9V/M60V apoC-II to analyze the extent of non-methionine specific oxidation occurring over the time course. This was observed to be quite minimal, with only ~6% detected after incubation for 1 h which increases to ~25% of non-methionine specific oxidation in the monomeric and fibrillar M9V/M60V sample after 72 h. To test the effect of this non-methionine specific oxidation on fibril formation by M9V/M60V apoC-II, stock solutions were incubated with H_2O_2 for 16 h and then diluted to a final concentration of 33 μM. Under these conditions, oxidized M9V/M60V apoC-II still readily assembles into amyloid fibrils with similar kinetics to wild-type apoC-II (see Supporting Information). This suggests that our observations for the dissociation of wild-type apoC-II fibrils are a specific effect of the oxidation of methionine residues within the fibrils.

DISCUSSION

In this study we have shown that oxidation of the methionine residues within apoC-II significantly inhibits its assembly into amyloid fibrils. Our findings are in good agreement with several other studies of amyloid-forming systems that also report inhibition of fibril formation following oxidation of one or more methionine residues (*27*−*30*). A key observation of our work is that the position of the oxidized methionine is important to its ability to inhibit fibrillogenesis. Oxidation of Met-60 located within the core fibril structural region of apoC-II inhibits fibril assembly, while oxidation of Met-9 which is outside this core region showed a much smaller effect (Figure 3). This is also demonstrated with M60Q substitutions that also significantly reduce the assembly of apoC-II fibrils (Figure 4), suggesting that the hydrophobic packing of side chains into cross-β structure is perturbed by this single amino acid change within the core region. Several other amyloidogenic proteins that are inhibited from fibril formation by methionine oxidation also have a key methionine residue located within their core fibril structural region. For Aβ in particular, Met-35 is positioned within the core fibril structural region (*44*), and oxidation of this residue inhibits fibril formation (*27*). A recent study using a designed ccβ-Met peptide provides an explanation as to why methionine oxidation can have such a significant effect on amyloid fibril formation (*45*). This work suggests that a certain number of site-specific hydrophobic interactions within the polypeptide chain are responsible for the formation of highly stable amyloid structure, and thus perturbation of one of these residues by the insertion of a single oxygen moiety has drastic effects on the kinetics and dynamics of fibril assembly (*45*). It is possible, therefore, that the presence of methionine residues located within

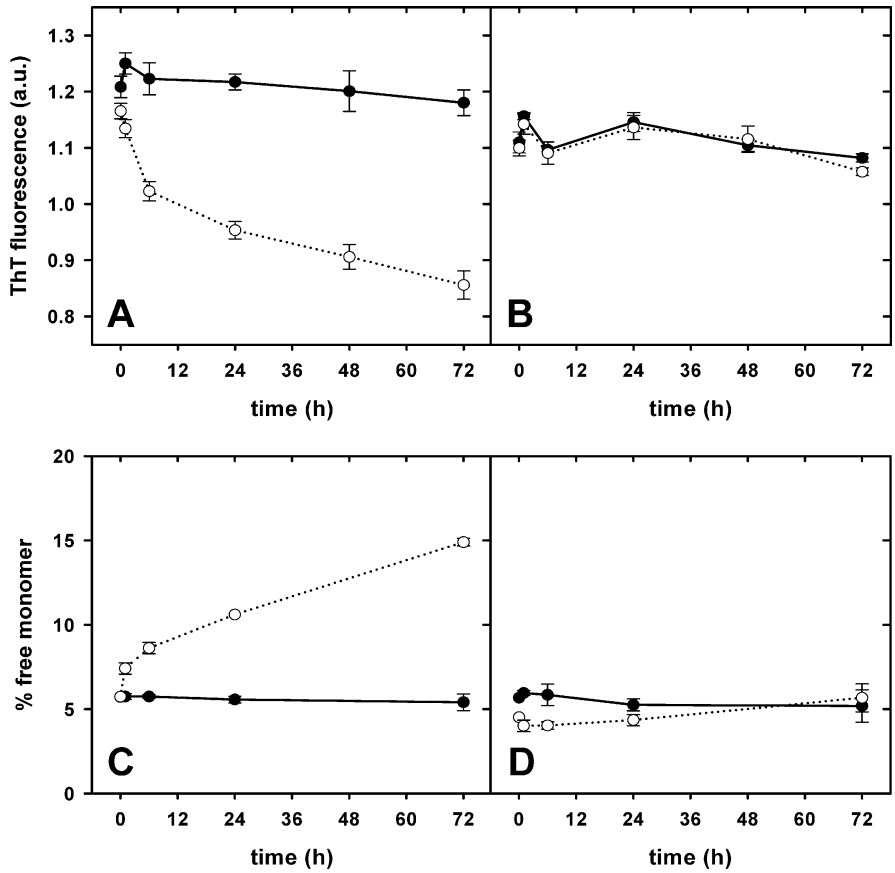

FIGURE 5: Treatment of preformed wild-type and valine-substituted apoC-II fibrils with hydrogen peroxide. Panels A and B: Fibrils of wild-type (panel A) and M9V/M60V (panel B) apoC-II were formed by incubation at room temperature at 33 μM for 7 days. After 168 h the fibrils formed were treated with 0.1% hydrogen peroxide (open symbols) and monitored by thioflavin T fluorescence for a further 72 h. Untreated fibrils were also monitored (closed symbols). Panels C and D: Hydrogen peroxide treated wild-type (panel C) and M9V/M60V (panel D) fibrils were also monitored by a pelleting assay to detect the change in free monomeric apoC-II over time (open symbols). Untreated fibrils were also monitored (closed symbols).

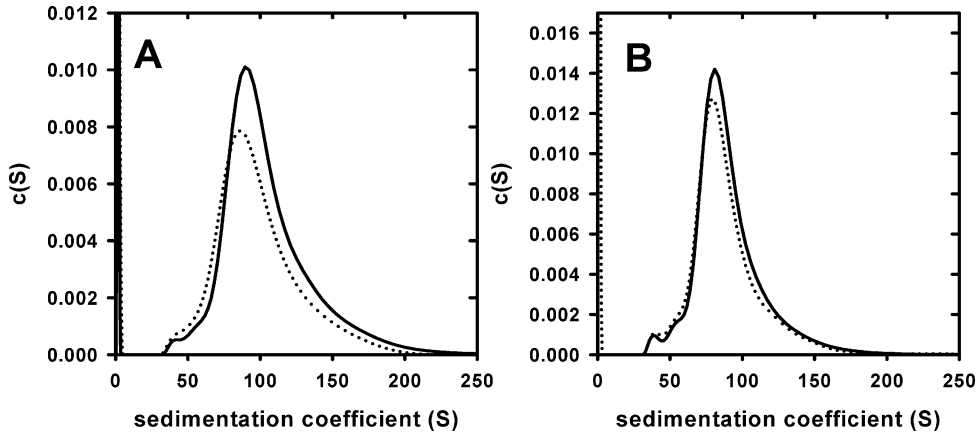

FIGURE 6: Sedimentation velocity analysis of hydrogen peroxide treated apoC-II fibrils. Wild-type fibrils (panel A) and M9V/M60V fibrils (panel B) were incubated with 0.1% hydrogen peroxide for 72 h (dotted lines) or left untreated as a control (solid lines).

specific core fibril regions provides an evolutionary mechanism designed to prevent amyloid fibril formation *in vivo.*

The ability to dissociate preformed apoC-II amyloid fibrils by treatment with hydrogen peroxide provides new information about the stability and dynamics of amyloid fibrils (Figure 6). The reversal of fibril assembly by this treatment shows that a simple change in the chemical nature of the polypeptide chain in the free monomeric pool or within the fibril can have drastic effects on the stability of the mature fibrils. The existence of a free pool of monomer has been shown in other amyloid fibril systems; for example, studies with Aβ peptide show a persistence of a small concentration of monomeric peptide at the completion of fibril formation (*46*). Also, fibrils formed from an SH3 domain coexist with a free monomeric pool that is in a constant recycling process involving a dissociation/reassociation mechanism (*47*). A recent study has shown that amyloid fibrils formed by lysozyme are able to be reversed by the application of increasing amounts of pressure to the system (*48*). Therefore, this study provides another example by which amyloid fibrils can be dissociated by a simple change in the physical conditions.

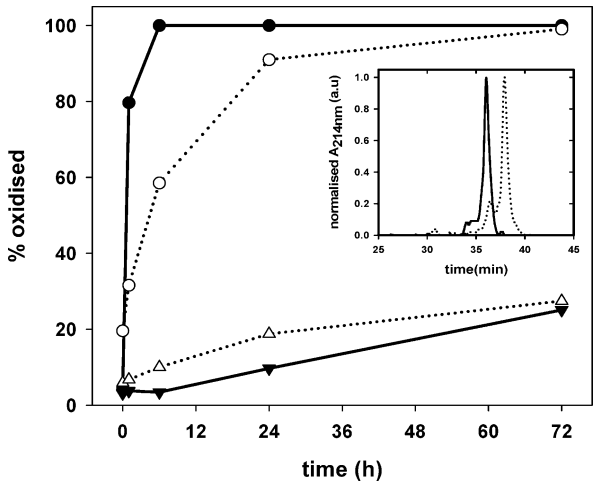

FIGURE 7: Extent of oxidation of monomeric and fibrillar apoC-II over time. Wild-type monomer (closed circles, solid lines) and fibrils (open circles, dotted line) were incubated with 0.1% hydrogen peroxide and analyzed by HPLC over time. The percentage of oxidized apoC-II was determined by fitting the HPLC profiles to a multiple Gaussian model using the program "PeakFit" to estimate the area under each peak. The difference in the total amount of "unoxidized peak" (elution time ~37.1 min) in the samples is plotted over time. The M9V/M60V monomer (closed triangles, solid lines) and fibrils (open triangles, dotted lines) were also analyzed to assess the amount of non-methionine specific oxidation over time. The inset shows the normalized HPLC profiles for wild-type fibrils (solid lines) and M9V/M60V fibrils (dotted lines) treated with H_2O_2 for 72 h.

The role that methionine residues play in the pathogenesis of amyloid disease remains poorly understood. Several studies have shown linkage of methionine residues to amyloid disease severity (*49*−*51*), and it remains plausible that among all of these different amyloid diseases there lies a common pathogenic mechanism. Several recent studies have sought to corroborate *in vitro* studies with oxidized amyloid-forming proteins with these *in vivo* observations. Bergstrom et al. show that the oxidation of a PrP peptide (106−126) has a potent inhibitory effect *in vitro* but also has enhanced toxicity *in vivo* (*33*). In addition, a study with a Met-Cys-substituted Aβ_{1-40} peptide shows that the fibrillogenesis of the mutated peptide is unaltered but cytotoxicity is reduced by the substitution of cysteine (*52*). The generation of ROS is a characteristic of many amyloid diseases, including Alzheimer's and cardiac amyloidoses (*53*−*55*), resulting in extensive oxidative damage to lipids, nucleic acids, and proteins (*56*). However, it is unclear how oxidative stress contributes to amyloid toxicity or whether it occurs as a result of amyloid fibril formation and deposition. With current debate in the field proposing prefibrillar soluble oligomers as the toxic species involved in amyloid disease pathogenesis (*16, 23*), it is possible that methionine oxidation may increase toxicity by reducing the rate and amount of fibrillogenesis of these proteins and, thus, enriching the amount of soluble toxic precursors. Thus, an increased understanding of the effect of methionine oxidation on the assembly and stability of mature fibrils will be essential in the development of therapeutics to treat these diseases.

ACKNOWLEDGMENT

We thank Dr. Yee-Foong Mok (Queens University, Canada) and Dr. Dennis Scanlon (Bio21 Institute, Melbourne, Australia) for provision of material.

SUPPORTING INFORMATION AVAILABLE

Further analysis of the assembly of apoC-II (wild type and M9V/M60V mutant) under oxidizing conditions and circular dichroism spectroscopy comparing the secondary structure of wild-type and M9Q/M60Q monomeric apoC-II. This material is available free of charge via the Internet at http://pubs.acs.org.

REFERENCES

1. Stadtman, E. R., and Levine, R. L. (2000) Protein oxidation. *Ann. N.Y. Acad. Sci. 899*, 191–208.
2. Vogt, W. (1995) Oxidation of methionyl residues in proteins: tools, targets, and reversal. *Free Radical Biol. Med. 18*, 93–105.
3. Jung, S., Hansel, A., Kasperczyk, H., Hoshi, T., and Heinemann, S. H. (2002) Activity, tissue distribution and site-directed mutagenesis of a human peptide methionine sulfoxide reductase of type B: hCBS1. *FEBS Lett. 527*, 91–94.
4. Kuschel, L., Hansel, A., Schonherr, R., Weissbach, H., Brot, N., Hoshi, T., and Heinemann, S. H. (1999) Molecular cloning and functional expression of a human peptide methionine sulfoxide reductase (hMsrA). *FEBS Lett. 456*, 17–21.
5. Koc, A., and Gladyshev, V. N. (2007) Methionine sulfoxide reduction and the aging process. *Ann. N.Y. Acad. Sci. 1100*, 383–386.
6. Moskovitz, J., Bar-Noy, S., Williams, W. M., Requena, J., Berlett, B. S., and Stadtman, E. R. (2001) Methionine sulfoxide reductase (MsrA) is a regulator of antioxidant defense and lifespan in mammals. *Proc. Natl. Acad. Sci. U.S.A. 98*, 12920–12925.
7. Levine, R. L., Mosoni, L., Berlett, B. S., and Stadtman, E. R. (1996) Methionine residues as endogenous antioxidants in proteins. *Proc. Natl. Acad. Sci. U.S.A. 93*, 15036–15040.
8. Taggart, C., Cervantes-Laurean, D., Kim, G., McElvaney, N. G., Wehr, N., Moss, J., and Levine, R. L. (2000) Oxidation of either methionine 351 or methionine 358 in alpha 1-antitrypsin causes loss of anti-neutrophil elastase activity. *J. Biol. Chem. 275*, 27258–27265.
9. Butterfield, D. A., Drake, J., Pocernich, C., and Castegna, A. (2001) Evidence of oxidative damage in Alzheimer's disease brain: central role for amyloid beta-peptide. *Trends Mol. Med. 7*, 548–554.
10. Chiti, F., and Dobson, C. M. (2006) Protein misfolding, functional amyloid, and human disease. *Annu. Rev. Biochem. 75*, 333–366.
11. Westermark, P., Benson, M. D., Buxbaum, J. N., Cohen, A. S., Frangione, B., Ikeda, S., Masters, C. L., Merlini, G., Saraiva, M. J., and Sipe, J. D. (2005) Amyloid: toward terminology clarification. Report from the Nomenclature Committee of the International Society of Amyloidosis. *Amyloid 12*, 1–4.
12. Dobson, C. M. (2002) Getting out of shape. *Nature 418*, 729–730.
13. Sipe, J. D. (1992) Amyloidosis. *Annu. Rev. Biochem. 61*, 947–975.
14. Selkoe, D. J. (2003) Folding proteins in fatal ways. *Nature 426*, 900–904.
15. Hardy, J. A., and Higgins, G. A. (1992) Alzheimer's disease: the amyloid cascade hypothesis. *Science 256*, 184–185.
16. Kayed, R., Head, E., Thompson, J. L., McIntire, T. M., Milton, S. C., Cotman, C. W., and Glabe, C. G. (2003) Common structure of soluble amyloid oligomers implies common mechanism of pathogenesis. *Science 300*, 486–489.
17. Walsh, D. M., Klyubin, I., Fadeeva, J. V., Cullen, W. K., Anwyl, R., Wolfe, M. S., Rowan, M. J., and Selkoe, D. J. (2002) Naturally secreted oligomers of amyloid beta protein potently inhibit hippocampal long-term potentiation in vivo. *Nature 416*, 535–539.
18. Lynch, T., Cherny, R. A., and Bush, A. I. (2000) Oxidative processes in Alzheimer's disease: the role of abeta-metal interactions. *Exp. Gerontol. 35*, 445–451.
19. Markesbery, W. R. (1997) Oxidative stress hypothesis in Alzheimer's disease. *Free Radical Biol. Med. 23*, 134–147.
20. Smith, D. G., Cappai, R., and Barnham, K. J. (2007) The redox chemistry of the Alzheimer's disease amyloid beta peptide. *Biochim. Biophys. Acta 1768*, 1976–1990.
21. Barnham, K. J., Ciccotosto, G. D., Tickler, A. K., Ali, F. E., Smith, D. G., Williamson, N. A., Lam, Y. H., Carrington, D., Tew, D., Kocak, G., Volitakis, I., Separovic, F., Barrow, C. J., Wade, J. D., Masters, C. L., Cherny, R. A., Curtain, C. C., Bush, A. I., and Cappai, R. (2003) Neurotoxic, redox-competent Alzheimer's beta-

amyloid is released from lipid membrane by methionine oxidation. *J. Biol. Chem. 278*, 42959–42965.
22. Gabbita, S. P., Aksenov, M. Y., Lovell, M. A., and Markesbery, W. R. (1999) Decrease in peptide methionine sulfoxide reductase in Alzheimer's disease brain. *J. Neurochem. 73*, 1660–1666.
23. Bucciantini, M., Giannoni, E., Chiti, F., Baroni, F., Formigli, L., Zurdo, J., Taddei, N., Ramponi, G., Dobson, C. M., and Stefani, M. (2002) Inherent toxicity of aggregates implies a common mechanism for protein misfolding diseases. *Nature 416*, 507–511.
24. Bemporad, F., Calloni, G., Campioni, S., Plakoutsi, G., Taddei, N., and Chiti, F. (2006) Sequence and structural determinants of amyloid fibril formation. *Acc. Chem. Res. 39*, 620–627.
25. Monsellier, E., Ramazzotti, M., de Laureto, P. P., Tartaglia, G. G., Taddei, N., Fontana, A., Vendruscolo, M., and Chiti, F. (2007) The distribution of residues in a polypeptide sequence is a determinant of aggregation optimized by evolution. *Biophys. J. 93*, 4382–4391.
26. Pawar, A. P., Dubay, K. F., Zurdo, J., Chiti, F., Vendruscolo, M., and Dobson, C. M. (2005) Prediction of "aggregation-prone" and "aggregation-susceptible" regions in proteins associated with neurodegenerative diseases. *J. Mol. Biol. 350*, 379–392.
27. Hou, L., Kang, I., Marchant, R. E., and Zagorski, M. G. (2002) Methionine 35 oxidation reduces fibril assembly of the amyloid abeta-(1−42) peptide of Alzheimer's disease. *J. Biol. Chem. 277*, 40173–40176.
28. Breydo, L., Bocharova, O. V., Makarava, N., Salnikov, V. V., Anderson, M., and Baskakov, I. V. (2005) Methionine oxidation interferes with conversion of the prion protein into the fibrillar proteinase K-resistant conformation. *Biochemistry 44*, 15534–15543.
29. Maleknia, S. D., Reixach, N., and Buxbaum, J. N. (2006) Oxidation inhibits amyloid fibril formation of transthyretin. *FEBS J. 273*, 5400–5406.
30. Uversky, V. N., Yamin, G., Souillac, P. O., Goers, J., Glaser, C. B., and Fink, A. L. (2002) Methionine oxidation inhibits fibrillation of human alpha-synuclein in vitro. *FEBS Lett. 517*, 239–244.
31. Collinge, J., Beck, J., Campbell, T., Estibeiro, K., and Will, R. G. (1996) Prion protein gene analysis in new variant cases of Creutzfeldt-Jakob disease. *Lancet 348*, 356.
32. Windl, O., Dempster, M., Estibeiro, J. P., Lathe, R., de Silva, R., Esmonde, T., Will, R., Springbett, A., Campbell, T. A., Sidle, K. C., Palmer, M. S., and Collinge, J. (1996) Genetic basis of Creutzfeldt-Jakob disease in the United Kingdom: a systematic analysis of predisposing mutations and allelic variation in the PRNP gene. *Hum. Genet. 98*, 259–264.
33. Bergstrom, A. L., Chabry, J., Bastholm, L., and Heegaard, P. M. (2007) Oxidation reduces the fibrillation but not the neurotoxicity of the prion peptide PrP106−126. *Biochim. Biophys. Acta 1774*, 1118–1127.
34. Medeiros, L. A., Khan, T., El Khoury, J. B., Pham, C. L., Hatters, D. M., Howlett, G. J., Lopez, R., O'Brien, K. D., and Moore, K. J. (2004) Fibrillar amyloid protein present in atheroma activates CD36 signal transduction. *J. Biol. Chem. 279*, 10643–10648.
35. Stewart, C. R., Haw, A., III, Lopez, R., McDonald, T. O., Callaghan, J. M., McConville, M. J., Moore, K. J., Howlett, G. J., and O'Brien, K. D. (2007) Serum amyloid P colocalizes with apolipoproteins in human atheroma: functional implications. *J. Lipid Res. 48*, 2162–2171.
36. Hatters, D. M., MacPhee, C. E., Lawrence, L. J., Sawyer, W. H., and Howlett, G. J. (2000) Human apolipoprotein C-II forms twisted amyloid ribbons and closed loops. *Biochemistry 39*, 8276–8283.
37. Binger, K. J., Pham, C. L., Wilson, L. M., Bailey, M. F., Lawrence, L. J., Schuck, P., and Howlett, G. J. (2008) Apolipoprotein C-II amyloid fibrils assemble via a reversible pathway that includes fibril breaking and rejoining. *J. Mol. Biol. 376*, 1116–1129.
38. Wang, C. S., Downs, D., Dashti, A., and Jackson, K. W. (1996) Isolation and characterization of recombinant human apolipoprotein C-II expressed in *Escherichia coli*. *Biochim. Biophys. Acta 1302*, 224–230.
39. Bohlen, P., Stein, S., Dairman, W., and Udenfriend, S. (1973) Fluorometric assay of proteins in the nanogram range. *Arch. Biochem. Biophys. 155*, 213–220.
40. Schuck, P. (2000) Size-distribution analysis of macromolecules by sedimentation velocity ultracentrifugation and Lamm equation modeling. *Biophys. J. 78*, 1606–1619.
41. MacRaild, C. A., Hatters, D. M., Lawrence, L. J., and Howlett, G. J. (2003) Sedimentation velocity analysis of flexible macromolecules: self-association and tangling of amyloid fibrils. *Biophys. J. 84*, 2562–2569.
42. Schuck, P., and Rossmanith, P. (2000) Determination of the sedimentation coefficient distribution by least-squares boundary modeling. *Biopolymers 54*, 328–341.
43. Wilson, L. M., Mok, Y. F., Binger, K. J., Griffin, M. D., Mertens, H. D., Lin, F., Wade, J. D., Gooley, P. R., and Howlett, G. J. (2007) A structural core within apolipoprotein C-II amyloid fibrils identified using hydrogen exchange and proteolysis. *J. Mol. Biol. 366*, 1639–1651.
44. Luhrs, T., Ritter, C., Adrian, M., Riek-Loher, D., Bohrmann, B., Dobeli, H., Schubert, D., and Riek, R. (2005) 3D structure of Alzheimer's amyloid-beta(1−42) fibrils. *Proc. Natl. Acad. Sci. U.S.A. 102*, 17342–17347.
45. Steinmetz, M. O., Gattin, Z., Verel, R., Ciani, B., Stromer, T., Green, J. M., Tittmann, P., Schulze-Briese, C., Gross, H., van Gunsteren, W. F., Meier, B. H., Serpell, L. C., Muller, S. A., and Kammerer, R. A. (2008) Atomic models of de novo designed ccbeta-Met amyloid-like fibrils. *J. Mol. Biol. 376*, 898–912.
46. O'Nuallain, B., Shivaprasad, S., Kheterpal, I., and Wetzel, R. (2005) Thermodynamics of abeta(1−40) amyloid fibril elongation. *Biochemistry 44*, 12709–12718.
47. Carulla, N., Caddy, G. L., Hall, D. R., Zurdo, J., Gairi, M., Feliz, M., Giralt, E., Robinson, C. V., and Dobson, C. M. (2005) Molecular recycling within amyloid fibrils. *Nature 436*, 554–558.
48. Abdul Latif, A. R., Kono, R., Tachibana, H., and Akasaka, K. (2007) Kinetic analysis of amyloid protofibril dissociation and volumetric properties of the transition state. *Biophys. J. 92*, 323–329.
49. Butterfield, D. A., and Bush, A. I. (2004) Alzheimer's amyloid beta-peptide (1−42): involvement of methionine residue 35 in the oxidative stress and neurotoxicity properties of this peptide. *Neurobiol. Aging 25*, 563–568.
50. Thylen, C., Wahlqvist, J., Haettner, E., Sandgren, O., Holmgren, G., and Lundgren, E. (1993) Modifications of transthyretin in amyloid fibrils: analysis of amyloid from homozygous and heterozygous individuals with the Met30 mutation. *EMBO J. 12*, 743–748.
51. Wadsworth, J. D., Asante, E. A., Desbruslais, M., Linehan, J. M., Joiner, S., Gowland, I., Welch, J., Stone, L., Lloyd, S. E., Hill, A. F., Brandner, S., and Collinge, J. (2004) Human prion protein with valine 129 prevents expression of variant CJD phenotype. *Science 306*, 1793–1796.
52. Dai, X. L., Sun, Y. X., and Jiang, Z. F. (2007) Attenuated cytotoxicity but enhanced betafibril of a mutant amyloid beta-peptide with a methionine to cysteine substitution. *FEBS Lett. 581*, 1269–1274.
53. Squier, T. C. (2001) Oxidative stress and protein aggregation during biological aging. *Exp. Gerontol. 36*, 1539–1550.
54. Huang, X., Moir, R. D., Tanzi, R. E., Bush, A. I., and Rogers, J. T. (2004) Redox-active metals, oxidative stress, and Alzheimer's disease pathology. *Ann. N.Y. Acad. Sci. 1012*, 153–163.
55. Stadtman, E. R., and Berlett, B. S. (1997) Reactive oxygen-mediated protein oxidation in aging and disease. *Chem. Res. Toxicol. 10*, 485–494.
56. Berlett, B. S., and Stadtman, E. R. (1997) Protein oxidation in aging, disease, and oxidative stress. *J. Biol. Chem. 272*, 20313–20316.

BI8009339